Brazilian Journal
of Chemical
Engineering

ISSN 0104-6632
Printed in Brazil

Vol. 21, No. 03, pp. 393 - 403, July - September 2004

NIOBIUM CARBIDE SYNTHESIS BY SOLID-GAS REACTION USING A ROTATING CYLINDER REACTOR

F. A. O. Fontes*, K. K. P. Gomes, S. A. Oliveira, C. P. Souza and J. F. Sousa

Universidade Federal do Rio Grande do Norte, Centro de Tecnologia, DEQ / PPGEQ e
DEM, Phone/Fax (84) 215-3760, 59072-970, Natal - RN, Brazil.
E-mail: franciscofontes@uol.com.br

(Received: March 15, 2002 ; Accepted: August 18, 2003)

Abstract - A rotating cylinder reactor was designed for the synthesis of niobium carbide powders at 1173 K. Niobium carbide, NbC, was prepared by carbothermal reduction starting from commercial niobium pentoxide powders. The reactor was heated using a custom-made, two-part, hinged, electric furnace with programmable temperature control. The design and operational details of the reactor are presented. The longitudinal temperature gradient inside the reactor was determined. Total reaction time was monitored by a gas chromatograph equipped with an FID detector for determination of methane concentrations. The results show that time of reaction depended on rotation speed. NbC was also prepared in a static-bed alumina reactor using the same conditions as in the previous case. The niobium carbide powders were characterized by X-ray diffraction and compared with commercially available products. Morphological, particle size distribution and surface area analyses were obtained using SEM, LDPS and BET, respectively. Therefore, the present study offers a significant technological contribution to the synthesis of NbC powders in a rotating cylinder reactor.
Keywords: rotating cylinder, reactor design, carbothermal reaction, niobium carbide, methane.

INTRODUCTION

The conventional industrial method (solid-solid diffusion) to produce niobium carbide (NbC) uses Nb_2O_5 and carbon at temperatures ranging between 1873 K and 2073 K with high energy consumption and long reaction times (Machado, 1996; Dal et al., 1993). However, previous work has shown that niobium pentoxide can be carburized from niobium monocarbide at 1173 K in a flux of CH_4-H_2 mixture, using static- bed reactors for small samples and under very well controlled conditions (Kim, 1999; Teixeira da Silva et al., 1996; Li et al., 1998; Souza et al., 1998).

Rotating cylinder reactors are used by metallurgical and chemical processing industries due to their versatility and ability to receive loads of particles of different sizes. A number of patents have been issued on the synthesis and processing of carbide, nitride and boride materials, mostly for commercial applications under development in small-scale operations or for theoretical aspects of heat transfer and material transport phenomena (Weimer, 1997; Carbolite, 1996; Roduit et al., 1996).

Rotating cylinder reactors can be easily controlled. These reactors reduce the sintering effect better and have larger gas/solid interfaces than static-bed reactors, which allows reduction of the excess gas reactant. Although rotating cylinder reactors have less gas/solid contact than fluidized bed reactors, they reduce the carry-over of fine particles in the exit of gases and require less gas reactant, since they do not require a minimum fluidization velocity. In addition, internal barriers disaggregate the material and result in the economical manufacture of products of uniform quality.

*To whom correspondence should be addressed

However, the development of models for industrial-scale applications can be complicated due to some restrictions on materials, maximum temperature and mechanical structures (Weimer, 1997). The rotary seals and thermal insulation systems at opposite ends of the reactor are important design challenges.

The objective of the present work is to present a prototype of a rotating cylinder reactor for NbC synthesis by gas-solid reaction using flowing CH_4/H_2. NbC was synthesized starting from Nb_2O_5 at different rotations. The same process was also carried out as a preliminary comparative study in a static bed alumina reactor under the same conditions of molar space speed, temperature and heating rate.

The Rotating Cylinder Reactor Design

The design of the rotating cylinder reactor was based on the following concepts:

1) The reactor material should be inert and stable to synthesize NbC in an atmosphere of CH_4-H_2 at temperatures around 1273 K.

2) The external diameter was adapted to the hinged chamber furnace diameter ($r_F = 0.02$ m) with the necessary adjustment (f).

$$r_e = r_F - f \tag{1}$$

3) To simplify loading and discharging, diameter holes ($d = 0.007$ m) were used to access the reactor central chamber.

4) To avoid material loss through the access holes, it was verified that the bed depth across the traverse section should be

$$h_{max} = \left(r - \frac{d}{2} \right) \tag{2}$$

where (r) is the internal radius of the reactor.

5) The recirculation pattern inside the cylinders without the occurrence of stagnation points was observed for a filling fraction (ψ) of (Wightman et al., 1998)

$$\psi = \frac{A_p}{A_r} \leq 0.36 \tag{3}$$

where (A_p) is the cross-sectional area filled with the precursor and (A_r) is the reactor internal cross-sectional area.

6) The reactor chamber should have walls thin enough to allow for quick heat transfer and also to offer good mechanical resistance and operational safety.

$$e = r_e - r \tag{4}$$

where (e) is the thickness of the chamber.

7) The degree of conversion ($F_c^* = 0.79$) from Nb_2O_5 to NbC was obtained as follows:

a) In a previous study (Teixeira da Silva et al., 1996), the transformation mechanism proposed for B-niobium pentoxide included a fast first step, corresponding to the reduction reaction ($B - Nb_2O_5 \rightarrow NbO_2$), and a slower second step, which consisted of the carburization of NbO_2 to NbC, through an unstable intermediate oxycarbide phase ($NbO_2 \rightarrow NbO_xC_y \rightarrow NbC$) revealed by X-ray photoelectron spectroscopy. However, the oxycarbide phase was not observable as a bulk phase by X-ray diffraction.

b) More recently, Kim et al. (1999) presented an approach based on thermogravimetric and chromatographic analysis and an X-ray diffraction pattern and described the stoichiometries of the two steps of Nb_2O_5 transformation as

For the first reduction step

$$Nb_2O_5 + H_2 \rightarrow 2NbO_2 + H_2O \tag{5}$$

For the reduction carburization step

$$NbO_2 + 3CH_4 \rightarrow NbC + 2CO + 6H_2 \tag{6}$$

c) Results from X-ray diffraction in samples obtained in the present study, by interruption of the reaction at intermediate reaction times, showed that only the Nb_2O_5, NbO_2 and NbC phases were observed, and therefore, the equations of Kim were selected to represent the transformation steps of Nb_2O_5 in NbC.

8) Based on the model used, the following parameters were calculated:

$$F_c = \frac{m_{NbC}}{m_{Nb_2O_5}} \tag{7}$$

$$\eta = \frac{F_c}{F_c^*} \cdot 100 \tag{8}$$

where (F_c) is the degree of solid conversion, (F_c^*) is the stoichiometric degree of solid conversion,

(m_{NbC}) is the mass of NbC, ($m_{Nb_2O_5}$) is the mass of Nb_2O_5 and (η) is the solid conversion efficiency.

9) The maximum loading of Nb_2O_5 ($m^*_{Nb_2O_5}$) by boatload was defined as 0.010 kg.

The Constructive Parameters

Figure 1 shows a cross-sectional view of the reactor chamber. The constructive parameters were obtained based on the precursor volume and its properties, using the MathCAD-Plus program for simulation and adjustment of the parameters. Starting from the reactor chamber dimensions and hinged furnace chamber, other design parameters were obtained using the software (Solid Edge) for CAD modeling.

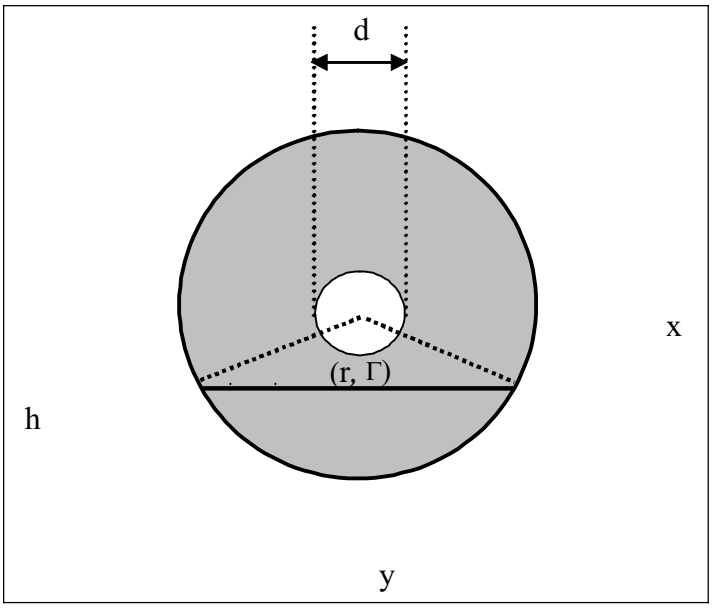

Figure 1: Reactor internal cross section. (h) bed depth, (r) internal radius, (Γ) completion angle and (d) diameter hole.

Data

$m^*_{Nb_2O_5} = 0.010 \text{ kg}$

$\rho^*_{Nb_2O_5} = 1330 \text{ kg.m}^{-3}$

$\psi = 0.36$

$r_e = 0.0160 \text{ m}$

$e = 0.0035 \text{ m}$

Resulting Parameters

$r = r_e - e$

$A_p = \psi(\pi.r^2)$

$$V_p = \frac{m^*_{Nb_2O_5}}{\rho^*_{Nb_2O_5}}$$

$$l = \frac{V_p}{A_p}$$

The parameters of the reactor chamber obtained were

$r_e = 0.0160 \text{ m}$

$r = 0.0125 \text{ m}$

$l = 0.0450 \text{ m}$

$V = 22 \times 10^{-6} \text{ m}^3$

Description of the Rotating Cylinder Reactor

Figures 2, 3 and 4 respectively illustrate the design of the rotating cylinder reactor, showing the assembly of the components, the rotary seals at opposite ends of the reactor and details of the reactor's central chamber with axial grooves used to disaggregate the reagent powders and the manufactured prototype.

Selection of Materials

The materials were selected according to theoperating temperature and atmosphere. Refractory stainless steel, Gerdau-316-L, was selected to make the reactor chamber and access tubes. This stainless steel contains 18 wt. % Cr and 14 wt. % Ni. It is suitable for continuous operation in a carbothermal reduction atmosphere of approximately 1173 K. The material is also erosion and oxidation resistant (Chiaverini, 1979; Gerdau, 1999). Polytetrafluorethylene (PTFE) was used for the rotary seals. This material is highly resistant to flame and water and it has a continuous heating resistance of approximately 533 K (Du Pont, 1999).

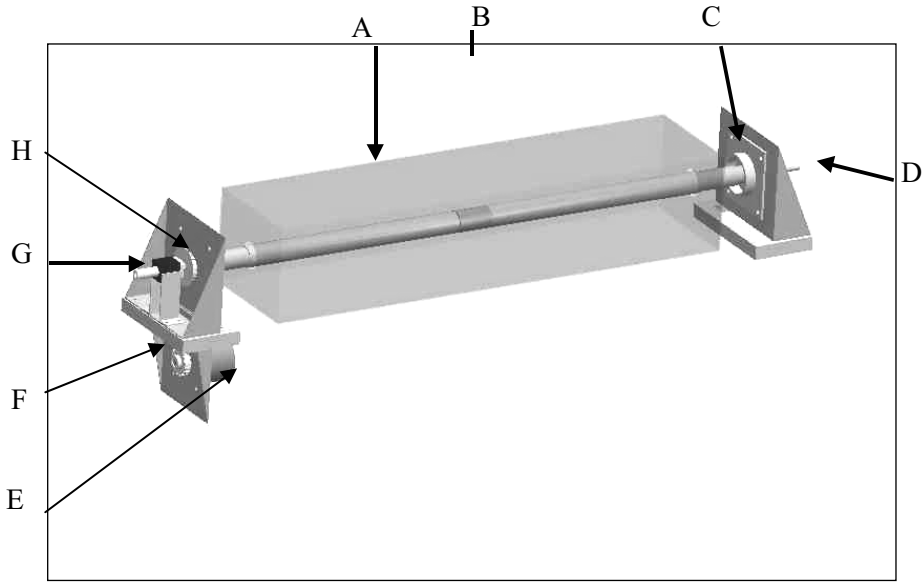

Figure 2: Rotating cylinder reactor assembly. (A) two-part, hinged, electric furnace, (B) reactor chamber, (C) bearings, (D) and (G) rotary seals, (E) step engine, (F) and (H) gears.

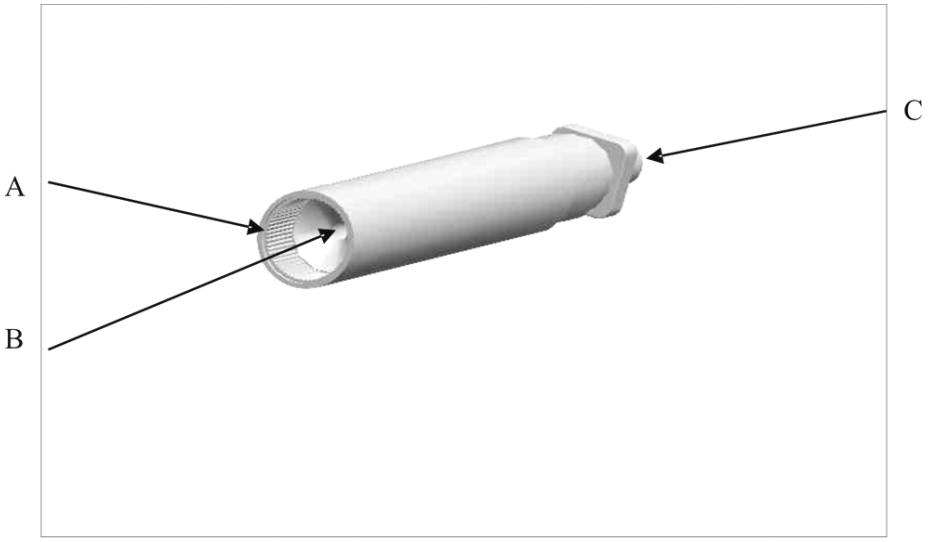

Figure 3: Reactor details. (A) reactor chamber, (B) access tube and (C) rotary seal.

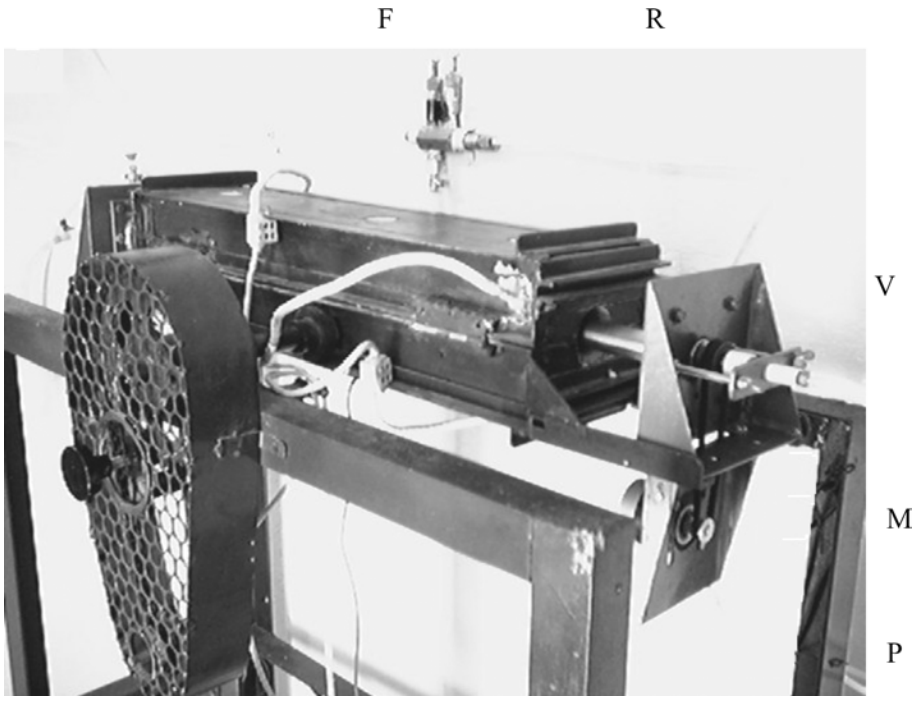

Figure 4: Prototype picture. (F) two-part, hinged, electric furnace, (P) device support, (R) rotating cylinder reactor, (M) step motor and (V) rotary seals.

EXPERIMENTAL

Methane (CH_4: 99.99%), hydrogen (H_2: 99.97%), and special argon in gaseous forms were obtained from AGA and synthetic air from White Martins (Recife-Brazil). All gases were passed through phosphorus pentoxide purifiers positioned in a line between the gas cylinders and the reactor. Niobium pentoxide (Nb_2O_5: 99.97%) and niobium carbide (NbC: 99 + %) were used as received from Alfa Aesar (Johnson Matthey Company, Miami, U.S.A.);

The carbides were first synthesized in a rotating cylinder reactor under the following conditions: commercial Nb_2O_5; $T = 1173$ K; $\beta = 0.1667$ K.s^{-1} up to 1173 K; $m_{Nb_2O_5} = 0.004$ kg; $V_p = 3\times10^{-6}$ m^3; $D_p = 20\times10^{-6}$ m; $z = 20\%$ (v/v); $Q = 2.2\times10^{-6}$ m^3.s^{-1}; $v = 0.0058$ s^{-1} and $n = 0$, 0.058, 0.083, 0.125 and 0.167 rps. Solid reactant boatload was delivered through a funnel inside the reactor and stopped with the pitch of (45 degree). Gaseous reactant mixtures were prepared using a J&W Scientific ADM-2000 volume flow meter. In an experiment, 0.004 kg of Nb_2O_5 was flowed with the reactant 20% (v/v) CH_4/H_2 while the reactor was heated by a two-part, hinged, electric furnace. The temperature was linearly increased from room temperature to the reaction temperature, controlled by a West Instruments N4400 temperature programmable controller and a thermocouple and using a heating rate of $\beta = 0.1667$ K.s^{-1}. Methane concentration during carburization was analyzed with a SRI 8610-C chromatographer equipped with an injection valve and an FID detector for methane adsorption analysis.

Total reaction time was measured when the peak of methane concentration returned to its initial position (Figure 6) and ten minutes later the oven was turned off. Then the CH_4/H_2 flux was substituted by an argon flux during the cooling down process, until the sample was removed from the reactor. The reactor continued rotating during the cooling down process and removal of the sample. The argon flux through the reactor was used to remove air from collecting glass. The powder samples obtained were removed with the reactor in an inclined position. After the powder sample was collected, the glass container was sealed to maintain an argon atmosphere. With this procedure the samples were not passivated.

A Siemens D-5000 X-ray diffractometer was used to characterize the powders obtained for the formation of crystalline samples. The BET analysis of the surface area was performed with a Nova-2000 analyzer, using nitrogen as adsorbate. The LDPS analysis of particle size distribution was performed with a Mastersizer S analyzer. The SEM analysis was also carried out with a Stereoscan 440. The

crystal particle diameter (D_c) was obtained by Debye-Scherrer`s formula (9) (Cullity, 1967), and assuming a spherical shape, the corresponding particle sizes (D_p) were calculated according to equation (10).

$$D_c = \frac{0.9\lambda}{B \cdot \cos\theta} \tag{9}$$

where (λ) is the wavelength of X-ray radiation (0.154 nm), (B) is the broadening of the diffraction line measured at half of its maximum intensity (radians) and (θ) is the Bragg angle.

$$D_p = \frac{6}{\left(S_g \cdot \rho\right)} \tag{10}$$

where (ρ) is the density of the solid and (S_g) is the specific surface area.

The NbC synthesis was also carried out in a static-bed alumina tube reactor with an internal radius of $r = 0.0170$ m using a cubic steel crucible (Stainless Steel-316) for placement of the solid reactant. The experimental conditions were the same as those used in the rotating cylinder reactor.

RESULTS AND DISCUSSION

The thermal gradient from the center to the end of the rotating cylinder reactor is shown in Figure 5. It can be seen that the temperature in the central chamber (reaction zone) remained constant. The internal temperature of the reactor steadily declined along the reactor length, reaching approximately room temperature at the ends, due to the thinner wails of the chamber at the ends than in the remainder of the reactor and the low coefficient of heat transfer of the Gerdau-316 stainless steel. The low temperature observed at the reactor ends was responsible for the durability of the Teflon rotary seals.

Methane adsorption in carbothermal reduction to form NbC is shown in Figure 6. The chromatograms obtained with peaksimple32 acquisition software (SRI Instruments) had similar characteristics for all experiments, where the final reaction time was defined as the point where the methane adsorption peak resumed its initial position. This was confirmed by X-ray diffraction analysis of the samples.

The rotational effect on the total reaction time of carbothermal reduction to form NbC in a rotating cylinder reactor is shown in Figure 7. It can be seen that the rotational effect produces a significant influence over the range of 0 to 0.083 rps and that above this range the influence is negligible. This activity is associated with bed transverse dissipation potency and its behavior agrees with Perron's model (Perron and Bui, 1994).

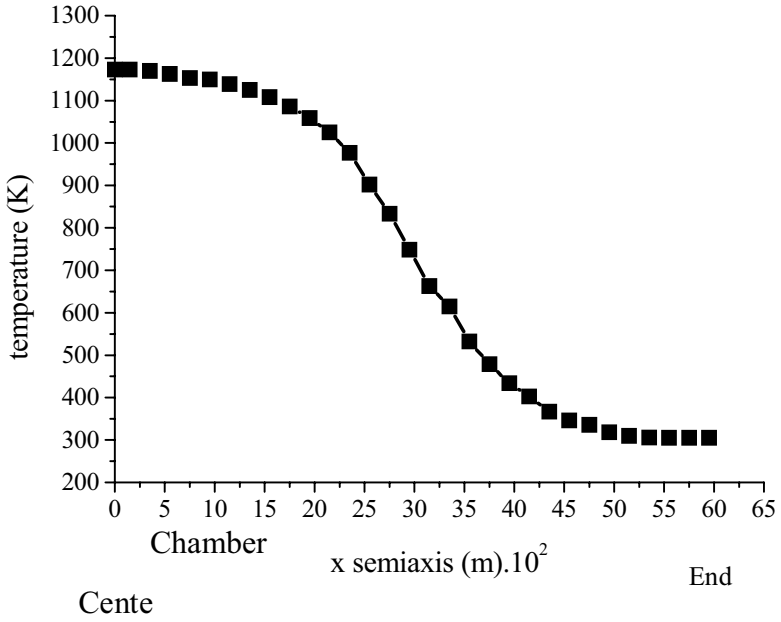

Figure 5: Thermal gradient from the center to the end of the rotating cylinder reactor.

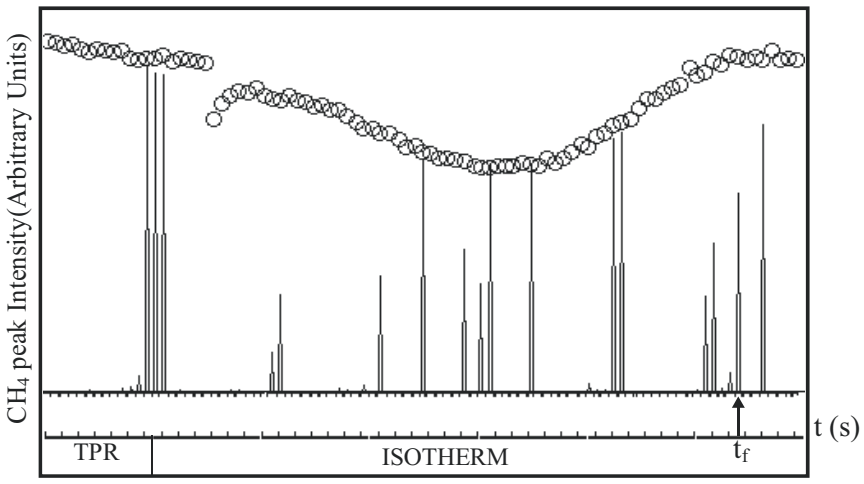

Figure 6: Methane adsorption chromatogram. (t_f) total reaction time, (TPR) temperature-programmed reaction zone and (ISOTHERM) isotherm zone.

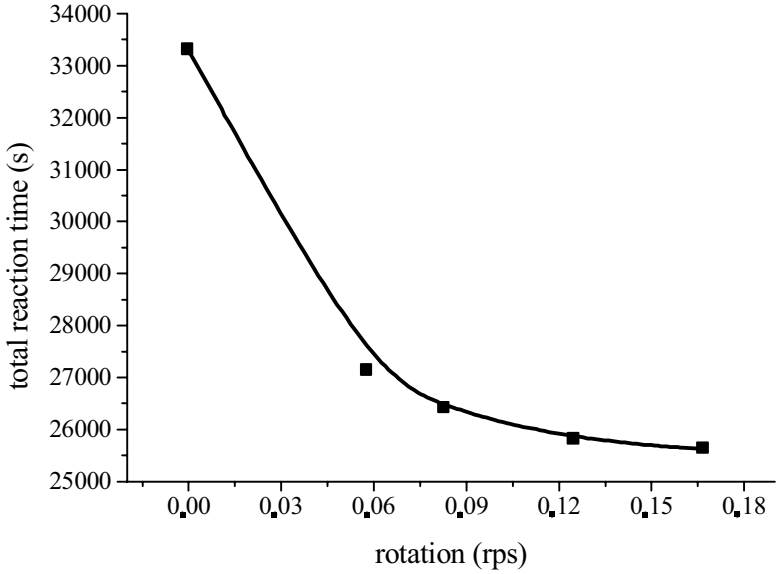

Figure 7: Effect of rotation speed on the total reaction time

The main characteristics of the synthesized carbide are reported and compared with those of commercial NbC in Table 1. The total reaction time with the rotating cylinder reactor fixed (0 rps) was shorter than the total reaction time obtained with the static-bed alumina reactor, due to the larger solid-gas interface area that improves diffusion through the rotating cylinder bed, in addition to the intense sintering effect on the synthesized carbide observed for the static-bed reactor. It was verified that the NbC crystal particle diameter changed slightly with the rotation, which could be mainly due to the low temperature used for the synthesis. This effect was significant when compared to NbC obtained from the static bed, because longer reaction times favor grain growth. The NbC crystal particle diameter obtained at 0.083 rps was 7% lower than that obtained for the static bed and 40% lower than that of the commercial NbC. The NbC crystal particle diameter (D_c) of the powder obtained in the rotating cylinder reactor for $z = 20\%$ (v/v), $n = 0.083$ rps, $T = 1173$ K, $v = 0.0085\ s^{-1}$ and $\beta = 0.1667\ K.s^{-1}$ was similar to that of the NbC obtained in a U-shaped quartz reactor by Teixeira da Silva et al. (1996) under the same conditions except $v = 0.1111\ s^{-1}$, as well as the results obtained by Kim et al. (1999) using a tubular quartz reactor for $z = 18\%$ (v/v), $T = 1123$ K, $v = 0.1000\ s^{-1}$ and $\beta = 0.0417\ K.s^{-1}$. The degree of solid conversion was reduced slightly with the rotation due to the carry-over of fine particles. This factor was larger in the static-bed alumina reactor

due to the smaller material losses during the loading and unloading procedures.

Figure 8 shows the particle size distribution for a commercial NbC and those obtained with the rotating cylinder reactor and static bed reactor, respectively. The results show that the commercial NbC had a smaller average particle size (15×10^{-6} m). The NbC processed in the rotating cylinder reactor at 0.083 rps, had an average particle size of 21×10^{-6} m, while the powders processed in the static-bed alumina reactor had a particle size of 30×10^{-6} m.

Figure 9 shows the X-ray diffraction patterns of NbC powders produced in the rotating cylinder reactor at 0 rps (Figure 9-(a)) and 0.167 rps (Figure 9-(b)) and in the static-bed alumina reactor (Figure 9-(c)) and that of a commercial NbC powder (Figure 9-(d)). The peaks correspond to the NbC JCPDS (Joint Committee on Powder Diffraction Standards) pattern. Other diffraction patterns had similar characteristics.

Figure 10 shows the morphology of NbC particles produced in the rotating cylinder reactor at 0.083 rps. The morphology of the NbC obtained from Nb_2O_5 in the rotating cylinder reactor shows a porous and uniform matrix.

Table 1: Main characteristics of the synthesized carbide.

n (rps)	S_g $(m^2kg^{-1}).10^{-3}$	Dc (m).10^9	Dp (m).10^9	t (s)	F_c (w/w)	η %
0.167	10.8	27	71	25200	0.749	94.8
0.083	11.2	28	69	25440	0.746	94.4
0.058	10.4	27	74	27000	0.750	94.9
0	10	26	77	31980	0.764	96.7
Static bed reactor	8.8	29	87	43200	0.780	98.7
Commercial NbC	13.7	45	56			
Commercial Nb_2O_5	1	45	1358			

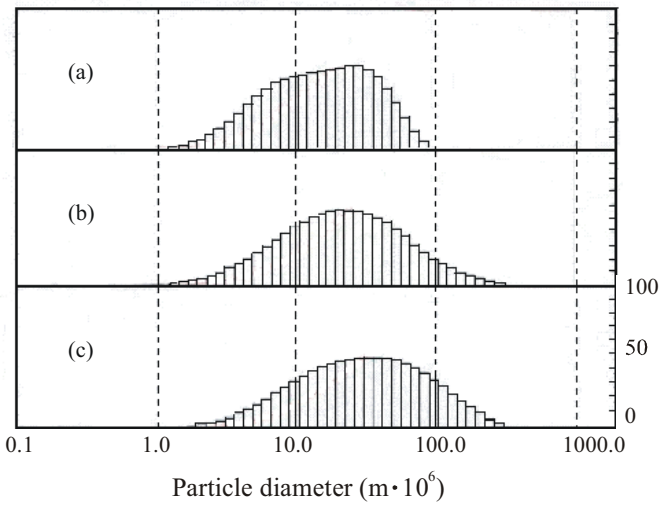

Figure 8: Particle size distribution. (a) Commercial NbC, (b) NbC obtained with the rotating cylinder reactor at 0.167 rps and (c) NbC obtained with the static-bed alumina reactor.

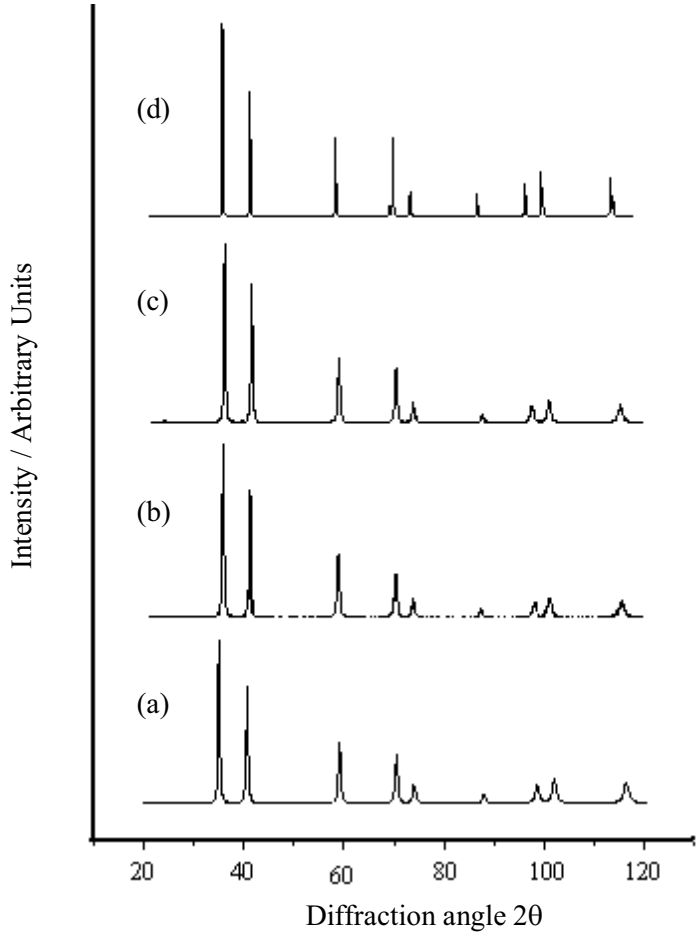

Figure 9: X-ray diffraction patterns of NbC. (a) 0 rps and (b) 0.167 rps in the rotating cylinder reactor, (c) static-bed alumina reactor and (d) commercial NbC.

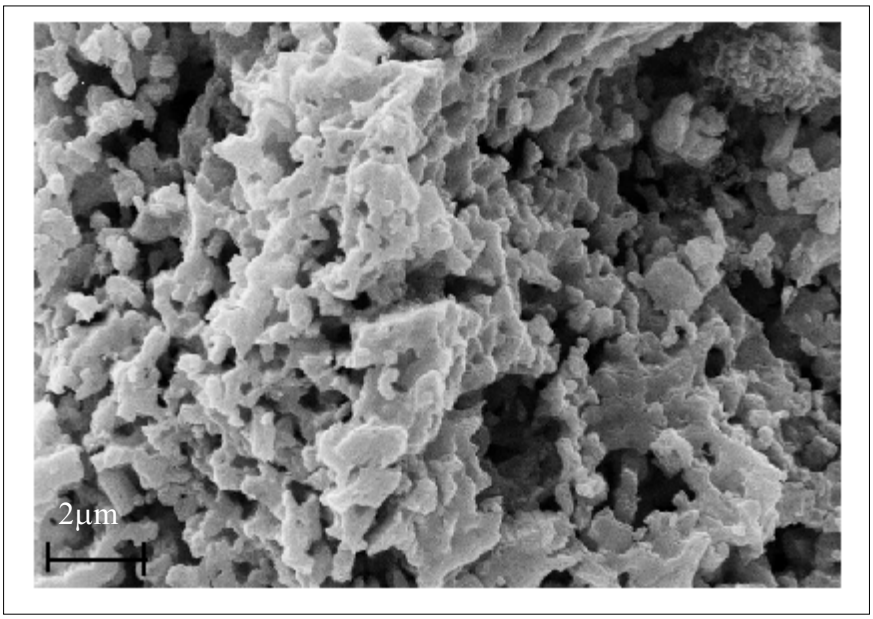

Figure 10: SEM picture of NbC obtained with the rotating cylinder reactor.

CONCLUSIONS

The experimental device, reactor and accessories produced NbC satisfactorily with ease of equipment handling and operational control, achieving the proposed objectives of this study.

It was possible to obtain NbC powders in a rotating cylinder reactor with a total reaction time of 25200 s, crystal particle diameter of $D_c = 27 \times 10^{-9}$ m, surface area of $S_g = 11 \times 10^3$ $m^2.kg^{-1}$, reaction temperature of $T = 1173$ K, heating rate of $\beta = 0.1667$ K s^{-1}, CH_4/H_2 rate of $z = 20$ % (v/v), molar space velocity of $v = 0.0058$ s^{-1} and rotation speed of $n = 0.083$ rps.

The results indicate that the rotational effect of the rotating cylinder reactor reduced substantially the total reaction time of carbothermal reduction of Nb_2O_5 to NbC. In addition, a reduction of the bed sintering effect allowed production of NbC powder. Processing in the static-bed alumina reactor required a longer reaction time and favored bed sintering. In all cases the degree of solid conversion and efficiency remained above 74 and 94 %, respectively. Optimization of the operational parameters and study of the carbothermal reduction kinetics are currently under way.

ACKNOWLEDGMENTS

We thank Mr. Frazão and Mr. Arivaldo, who work in the Nucleo Tecnologico Industrial – UFRN, for their technical support and Prof. Fontes, Lúcio A. O. and Prof. Fernandes, Joana D'Arc G. for their collaborative work. We would also like to thank the BRASINOX industry staff, the Chemical Engineering Graduate Program–UFRN-Natal and the CNPq Scholarship Program for undergraduate students, the LSR-UFPB Laboratório de Solidificação Rápida, the LCT-EP-USP Laboratório de Caracterização Tecnológica and LATMAT-UFRN Laboratório de Análise Térmica e Materiais.

NOMENCLATURE

A_p	area of the cross section filled with the precursor (m^2)
A_r	internal cross-sectional area of the reactor (m^2)
d	hole diameter (m)
D_c	crystallite size (m)
D_p	particle size (m)
e	thickness of the reactor chamber wall (m)
f	factor of correction between r_F and r_e
F_c^*	stoichiometric degree of solid conversion
F_c	degree of solid conversion
h_{max}	maximum bed depth (m)
l	reactor chamber length (m)
$m^*_{Nb_2O_5}$	maximum mass of Nb_2O_5 (kg)
$m_{Nb_2O_5}$	mass of Nb_2O_5 (kg)
m_{NbC}	mass of NbC (kg)
n	rotation speed (rps)
Q	CH_4-H_2 flow (m^3 s^{-1})
r	reactor internal radius (m)
r_e	reactor external radius (m)
r_F	furnace radius (m)
S_g	surface area (m^2 kg^{-1})
t	reaction time (s)
t_f	total reaction time (s)
T	temperature (K)
V_p	volume of precursor reagent (m^3)
V_r	volume of reactor chamber (m^3)
z	CH_4/H_2 ratio (%)
β	heating rate (K s^{-1})
Γ	completion angle (rd)
ρ	density of the solid
$\rho^*_{Nb_2O_5}$	apparent specific mass of the Nb_2O_5 (kg m^{-3})
v	molar space velocity (s-1)
ψ	fill fraction
η	solid conversion efficiency (%)

REFERENCES

Carbolite, Rotary Reactor Furnace. Keison International Plc. (1996).

Chiaverini, V., Aços e Ferros Fundidos. 4th ed., São Paulo: ABM (1979).

Cullity, B.D., Elements of X-Ray Diffraction. Addison-Wesley Publishing Company. 514 pg. USA (1967).

Dal, B.F., Hardin, S.G., Hay, D.G. and Turney, T.W., Selective, Low-Temperature Syntheses of Niobium Carbide and a Mixed (Niobium/Tungsten) Carbide from Metal Oxide-Polyacrylonitrile Composites by Carbothermal Reduction. Journal of Material Science, Victoria: Chapman & Hall, 28, 6657-6664 (1993).

Du Pont, E.I, Catálogo de Politetrafluoretileno (Teflon). São Paulo: Du Pont (1999).

Gerdau, Catálago de Aços Inoxidáveis. São Paulo: Gerdau (1999).

Kim, H.S., Bugli, G. and Djéga-Mariadassou, G., Preparation and Characterization of Niobium Carbide and Carbonitride. Journal of Solid State Chemistry, 142, 100-107 (1999).

Li, J.-B., Xu, G.-Y., Sun, E.Y., Huang, Y. and Becher, P.F., Synthesis and Morphology of Niobium Monocarbide Whiskers. Journal of American Ceramic Society, Westerville: Amer. Cerm. Soc., 81, 1689-1691 (1998).

Machado, T.G., Obtenção de Carbetos de Nióbio. 63p. Master's thesis, Universidade Federal do Rio Grande do Norte, Natal. (1996).

Perron, J. and Bui, R.T., Fours Rotatifs: Modèle Dynamique du Mouvement du Lit. The Canadian Journal of Chemical Engineering, 72, 16-25 (1994).

Roduit, B., Maciejewski, M. and Baiker, A., Influence of Experimental Conditions on the Kinetic Parameters of Gas-Solid Reactions - Parametric Sensitivity of Thermal Analysis. Thermochimica Acta. Elsevier Science, 282/283, 101-119 (1996).

Souza, C.P., Medeiros, F.F.P., Satre, P., Roubin, M., Preparation of Niobium Carbide from an Organometallic Precursor, In: Chisa 98, Praha – Czech Republic (1998).

Teixeira da Silva, V.L.S., Schmal, M., Oyama, S.T., Niobium Carbide Synthesis from Niobium Oxide: Study of the Synthesis Conditions, Kinetics, and Solid-State Transformation Mechanism. Journal of Solid State Chemistry, Academic Press, 123, 168-182 (1996).

Weimer, A.W., Carbide, Nitride and Boride Materials Synthesis and Processing. Ed. Chapman & Hall, New York, 671p. (1997).

Wightman, C., Moakher, M. and Muzzio, F.J., Simulation of Flow and Mixing of Particles in a Rotating and Rocking Cylinder. AIChe Journal, 44, 1266-1276 (1998).